Artificial intelligence models deployed at scale on hematoxylin and eosin-stained whole slide images reveal stage-dependent collagen composition in metabolic dysfunction-associated steatohepatitis

Ylaine Gerardin[1], Neel Patel[1], Lara Murray[1], Adam Stanford-Moore[1], Jacqueline Brosnan-Cashman[1], Jun Xu[2], Lisa Boyette[2], Benjamin Glass[1], Timothy R. Watkins[2], Andrew Billin[2], Robert Egger[1]

[1]PathAI, Boston, Massachusetts, USA; [2]Gilead Sciences, Inc., Foster City, California, USA

Poster #THU-261

STUDY BACKGROUND

- Diagnosis and staging of metabolic dysfunction-associated steatohepatitis (MASH; formerly NASH) currently requires manual pathologist identification of fibrotic structures on collagen-stained slides. The qualitative assessment of these structures makes MASH staging prone to inter-rater variability [1]. More granular, quantitative histopathologic assessment could inform the understanding of fibrosis progression and regression in MASH.
- We developed AI models to detect and quantify fibrotic features from scanned hematoxylin and eosin-stained (H&E) whole slide images (WSI) at scale and used the results to characterize fibrosis composition in MASH biopsies.

METHODS

Liver Explore ML Models

- Ordinal and continuous ML-derived MASH CRN scores for each sample were generated via the AI-based Measurement of MASH Histology tool (AIM-MASH+™,^ [2]; **Figure 1**).
- We trained an ML model to detect histological landmarks (portal tracts and central veins) in WSI of H&E-stained MASH biopsies based on manual pathologist annotations. We also trained an ML model to detect collagen in H&E biopsies [3] and classify it as one of multiple structural or pathological categories. This suite of models (**Liver Explore***) is depicted in **Figure 2**.
- The resulting models were deployed alongside previously developed ML-based models [4,5] that identify different hepatocytes and immune cell subtypes, as well as regions of steatosis, lobular inflammation and hepatocellular ballooning to characterize tissue composition.
- Over 1,000 HIFs, including tissue and fibrosis areas, cell counts and densities, were extracted per WSI to quantitatively and exhaustively characterize tissue and cell micro-architecture.

Figure 1. AIM-MASH+ CRN ordinal and continuous scoring.

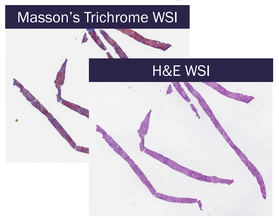

	Ordinal CRN Grade/Stage	Continuous Score
Fibrosis stage	4	4.2
Ballooning grade	2	3.0
Steatosis grade	2	2.3
Lobular Inflammation grade	2	2.9

Datasets

- Models were deployed on WSIs from patients enrolled in the STELLAR-3 (NCT03053050; N=1679) and STELLAR-4 (NCT03053063; =1898) clinical trials, which enrolled patients with F3 and F4 fibrosis, respectively [6]. Clinical metadata was available for all evaluated patients.

Analysis

- We characterized the patient populations enrolled in STELLAR-3 and STELLAR-4 by using ordinal and continuous CRN scores of fibrosis, relating them to HIFs associated with collagen composition.

STUDY OVERVIEW

Figure 2. Example of Liver Explore* outputs on a WSI of an H&E biopsy

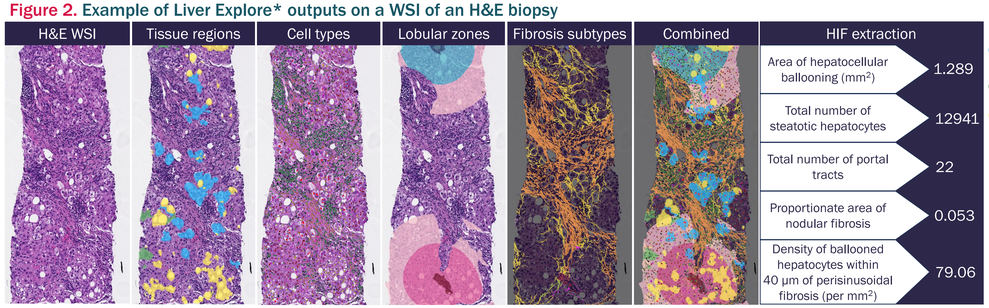

Model-identified tissue regions, cell types, lobular zones, and collagen and fibrosis subtypes are superimposed on each H&E image.

Figure 3. Classification of collagen and fibrosis subtypes identified by Liver Explore

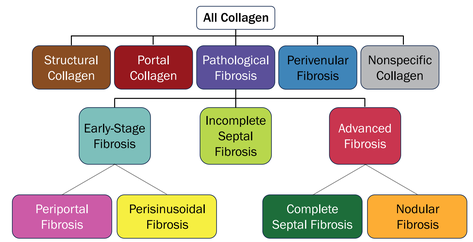

RESULTS

- AI-based fibrosis quantification revealed an increase in total collagen, pathological fibrosis, and advanced fibrosis (e.g., nodular fibrosis) with CRN fibrosis stage (**Figure 4**).
- Dimensionality reduction revealed manually-staged F0, F1, and F2 subpopulations to be highly overlapping in the first two principal components, which accounted for 67% of total sample variation (**Figure 5A**). Nodular fibrosis drives the first component of greatest variation across the samples, separating out F4 at the highest extreme and F3 samples at intermediate values (**Figure 5B**).
- ML-predicted continuous fibrosis (cFib) scores, inclusive of subordinal stages, are associated with appreciable changes in tissue architecture (**Figure 6**). Advanced and nodular fibrosis increase rapidly at cFib >3, while early-stage (perisinusoidal and periportal) as well as incomplete septal fibrosis decrease (**Figure 6A-B**). Inflammation in highly fibrotic and cirrhotic patients is reflected in an increased density of immune cells for cFib >3, accompanied by a decrease in all types of hepatocytes (**Figure 6C-D**).

Figure 4. Classification of collagen composition by CRN fibrosis stage.

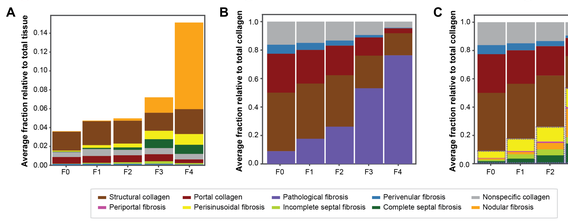

Relative area of all predicted fibrosis subtypes were assessed.

A) The fraction of fibrosis subtypes relative to total tissue reveals increased total collagen and increased nodular fibrosis with increased CRN fibrosis stage.
B) The relative fraction of total collagen classified as pathological fibrosis increases in a step-wise fashion with CRN fibrosis score.
C) Further sub-classifying pathological fibrosis (purple box) reveals the observed increase in pathological fibrosis is largely due to nodular fibrosis.

Figure 5. Contributions of fibrosis subtypes to CRN fibrosis stage.

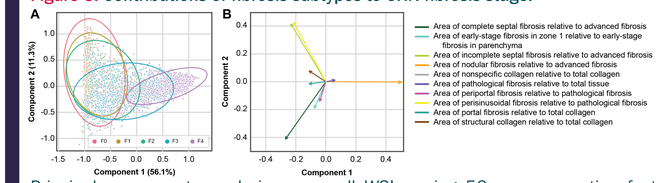

Principal components analysis across all WSIs, using 56 area proportion features relating to fibrosis subtypes.

A) Projection of WSI onto first two PCs, colored by manual fibrosis stage. F4 and F3 cases show clear distinction from F0, F1, and F2 cases.
B) Arrows indicating the top feature loading for each fibrosis subtype are shown. Features relating to nodular fibrosis drove the first component of greatest variation across the samples.

Figure 6. Collagen subtypes and cell composition changes with increasing continuous fibrosis score.

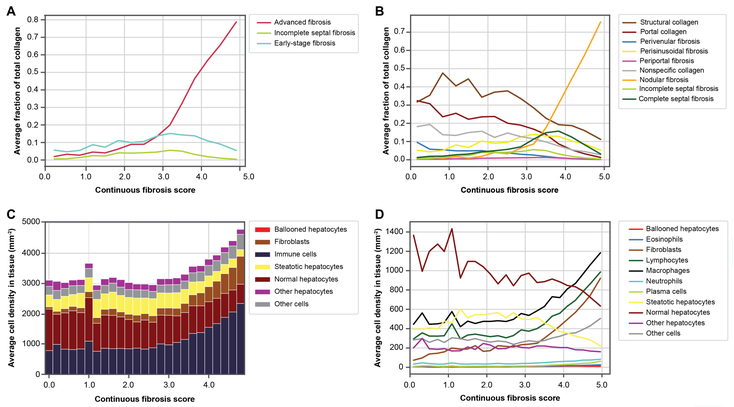

Liver Explore-predicted fibrosis subtypes (A-B) and cell types (C-D) were assessed as a function of AIM-MASH+ cFib scores, revealing an association between subordinal fibrosis stages and tissue architecture.

A) At cFib >3, advanced fibrosis increases sharply. At scores lower than this inflection point, early-stage and incomplete septal fibrosis increase slightly, then decrease as fibrosis score increases.
B) At cFib >3, nodular fibrosis increases sharply. At this point, perisinusoidal and incomplete septal fibrosis begin to decrease. Relative amounts of structural collagen, portal collagen, and nonspecific collagen all decrease as cFib score increases.
C) At cFib >3, the relative number of immune cells and fibroblasts increases.
D) The observed increase in immune cells in cFib > 3 is due largely to increased levels of macrophages and lymphocytes. Both normal and steatotic hepatocytes decrease in frequency in cFib >3, as well.

CONCLUSIONS

- Characterization of pathological fibrosis and non-pathological collagen features via AI digital pathology yields understanding of MASH fibrosis progression beyond the resolution provided by CRN scoring.
- The presence of expected associations, such as nodular fibrosis in F4, provides biological support for empirically-validated AI fibrosis staging.
- Quantifying fibrosis directly from scanned H&E images with Liver Explore requires no custom microscopy and is scalable for applications in drug development, enhancing understanding of therapeutic mechanisms for anti-fibrotic drugs, and potentially use in clinical care.

CONTACT

Lara Murray: lara.murray@pathai.com
publications@pathai.com

REFERENCES

1) Davison, BA, et al. (2020) *J Hepatol.* 73(6):1322-1332.
2) Iyer, JS, et al. *medRxiv*. doi: https://doi.org/10.1101/2023.04.20.23288534
3) Zhang, Y, et al. (2023) *Hepatology.* 78(S1): S835.
4) Mistry, P, et al. (2023) *Hepatology* 78(S1): S790.
5) Carrasco-Zevallos, O, et al. *Hepatology*. 75(2): S254.
6) Harrison, SA, et al. (2018) *Gastroenterology.* **155: 1140-1153.**

* Liver Explore is for research use only. Not for use in diagnostic procedures.
^ AIM-MASH+ is for research use only. Not for use in diagnostic procedures.

ACKNOWLEDGMENTS

We would like to thank the patients enrolled in STELLAR-3 and STELLAR-4 and their families. We would also like to thank the members of PathAI Pathology Network who contributed towards this work.

This poster template was developed by SciStories LLC. https://scistories.com/

EASL International Liver Congress; June 5-8, 2024; Milan, Italy